J. Phase Equilib. Diffus. (2019) 40:686–696
https://doi.org/10.1007/s11669-019-00755-7

Diffusion Research in BCC Ti-Al-Zr Ternary Alloys

Fujun Fan[1] · Yuanyu Gu[1,2] · Guanglong Xu[1] · Hui Chang[1] · Yuwen Cui[1,2]

Submitted: 1 June 2019 / in revised form: 25 August 2019 / Published online: 23 September 2019

Abstract Diffusion behavior in the BCC Ti-Al-Zr ternary alloys was experimentally investigated at 1273 K (1000 °C) and 1473 K (1200 °C) by means of the diffusion-couple technique. Upon the Whittle-Green and generalized Hall methods, the inter- and impurity diffusion coefficients were respectively extracted from the composition profiles acquired by the electron microprobe analysis (EPMA) and subsequently represented by the error function expansion. The extracted main interdiffusion coefficient $\tilde{D}^{\mathrm{Ti}}_{\mathrm{AlAl}}$ increases with increasing the content of either Al or Zr, and the increase is appearing more considerably at the higher temperature. However, $\tilde{D}^{\mathrm{Ti}}_{\mathrm{ZrZr}}$ was noticed to decrease with the increase of Al and Zr contents at 1273 K (1000 °C) while there is an upward trend at 1473 K (1200 °C). The impurity diffusion coefficients of Al in Ti-Zr binary alloys, $D^{*}_{\mathrm{Al(Ti-Zr)}}$, and of Zr in Ti-Al binary alloys, $D^{*}_{\mathrm{Zr(Ti-Al)}}$, increase with increasing the Zr and Al contents respectively. A comparison of average main interdiffusion coefficient $\overline{\tilde{D}^{\mathrm{Ti}}_{\mathrm{XX}}}$ made among ten Ti-Al-X ternary systems suggests that the Zr diffusion is most comparable to Cr and could operate via a vacancy-controlled mechanism.

Keywords generalized Hall method · impurity diffusion · interdiffusion · Ti-Al-Zr BCC ternary alloys · Whittle-Green method

1 Introduction

Titanium and its alloys have increasing applications in aerospace, automotive and marine industries due to their high specific strength, excellent mechanical properties and good corrosion resistance.[1–3] Most commercial titanium alloys are complex and multicomponent in nature. Representative Ti alloys include Ti-6321,[4] Ti-7333,[5] Ti-55531,[6] and Ti-B19,[7] etc., which are principally alloyed with elements classified as α (HCP), β (BCC), or neutral stabilizers. The α stabilizing element Al practically enhances the tensile and the creep strength while it reduces the density, whereas the neutral element Zr is typically used as solid-solution strengthener to improve corrosion resistance, processability, and weldability.[8,9] The knowledge-driven optimization of the mechanical properties of complex titanium alloys are essentially the control of intricate microstructures through such processes and transformations as recovery, recrystallization, grain growth, and precipitation, all of which are more or less governed by the diffusion phenomena. In fact, accurate diffusion properties also serve as the fundamental kinetic data for mesoscale modeling of microstructural evolution[10] and macroscale modeling of solidification process.[11]

So far, the diffusion properties of BCC Ti-Al[12,13] and Ti-Zr[14] binary alloys have received attention, however, the diffusion in BCC Ti-Al-Zr ternary alloys has been yet addressed. Therefore, the objectives of the present work are to investigate the interdiffusion behaviors of BCC Ti-Al-Zr

Fujun Fan and Yuanyu Gu have contributed equally to this work.

✉ Yuwen Cui
ycui@unizar.es

[1] Tech Institute for Advanced Materials and School of Materials Science and Engineering, Nanjing Tech University, Nanjing 210009, People's Republic of China

[2] Instituto de Ciencia de Materiales de Aragon (ICMA), Zaragoza 50009, Spain

ternary alloys at 1273 K (1000 °C) and 1473 K (1200 °C), and to extract the inter- and impurity ternary diffusion coefficients, respectively.

2 Materials and Methods

2.1 Experimental Procedure

Fourteen binary and six ternary alloys were prepared from 99.9 wt.% sponge pure Ti, 99.99 wt.% Al and 99.9 wt.% Zr pure granules by induction melting under an argon atmosphere. The actual compositions of the alloys are listed in Table 1. All the compositions of the alloys were designed to locate in the BCC phase region of Ti-Al-Zr system at both 1273 K (1000 °C) and 1473 K (1200 °C) according to the accepted phase diagrams.[15] The melting was repeated six times to attain a homogeneous composition.

The alloy ingots were then solid-solution treated under vacuum in quartz tubes at 1473 K (1200 °C) for 10 h followed by water quenching, which resulted in the alloys with average grain size larger than 1 mm such that the effect of grain boundary diffusion could be neglected. Small rectangular blocks with a size 9 × 9 × 5 mm were cut from the annealed ingots. One of the wide surfaces of the blocks were polished to mirror-like quality. The well-contacted diffusion couples were assembled with appropriate pairs by diffusion-bonding under vacuum (10^{-3}Pa) at 1173 K (900 °C) for 4 h by using a stainless steel bonding jig, during which tantalum foil was placed between the couple and the jig to avoid the contamination. The assembled diffusion couples were then capsuled into quartz tubes, evacuated and back-flashed with argon, annealed under predetermined conditions (refer to Table 1 for the temperatures and times of long-term interdiffusion annealing), and quenched into cold water. The diffusion couples were sectioned along the diffusion direction which suffered no potential oxidation and evaporation of elements, and prepared by standard metallographic technique. The microstructures of diffusion zone of the diffusion couples were characterized by scanning electron microscopy (SEM) and the local compositions along the diffusion direction were analyzed by electron microprobe analysis (EPMA, JEOL JAX-8230).

2.2 Extraction of Diffusion coefficients

Figure 1 presents the backscattered electron (BSE) image of diffusion couple A7 at 1273 K (1000 °C) for 48 h and the composition profiles of Al and Zr obtained by the EPMA measurements. To avoid the point-to-point fluctuation of the experimental data and the errors introduced during the fitting or smoothing, the error function expansion (ERFEX)[16–19] was used to represent the composition profiles acquired by EPMA with analytical form:

Table 1 Actual terminal compositions of Ti-Al-Zr diffusion couples (at.%)

Temperature, K	Diffusion time, h	Diffusion couples	Compositions, at.%
1273	48	A1	Ti-1Al/Ti-4.4Zr
		A2	Ti-2.8Al/Ti-4.3Zr
		A3	Ti-2.8Al/Ti-9.9Zr
		A4	Ti-5.1Al/Ti-13.5Zr
		A5	Ti-5.5Al/Ti-19.9Zr
		A6	Ti-5.5Al/Ti-28.2Zr
		A7	Ti/Ti-9.5Al-39.5Zr
		A8	Ti/Ti-11.2Al-20.1Zr
		A9	Ti-2.8Al/Ti-11.6Al-19.6Zr
1473	17	B1	Ti-2.6Al/Ti-4.3Zr
		B2	Ti-5.2Al/Ti-4.4Zr
		B3	Ti-5.2Al/Ti-8.7Zr
		B4	Ti-8.8Al/Ti-12.9Zr
		B5	Ti-14.2Al/Ti-19.9Zr
		B6	Ti-19.5Al/Ti-28.7Zr
		B7	Ti-14.8Al/Ti-38.4Zr
		B8	Ti-19.5Al/Ti-38.4Zr
		B9	Ti/Ti-9.7Al-36.3Zr
		B10	Ti/Ti-12.3Al-19.2Zr
		B11	Ti/Ti-14.5Al-11.4Zr

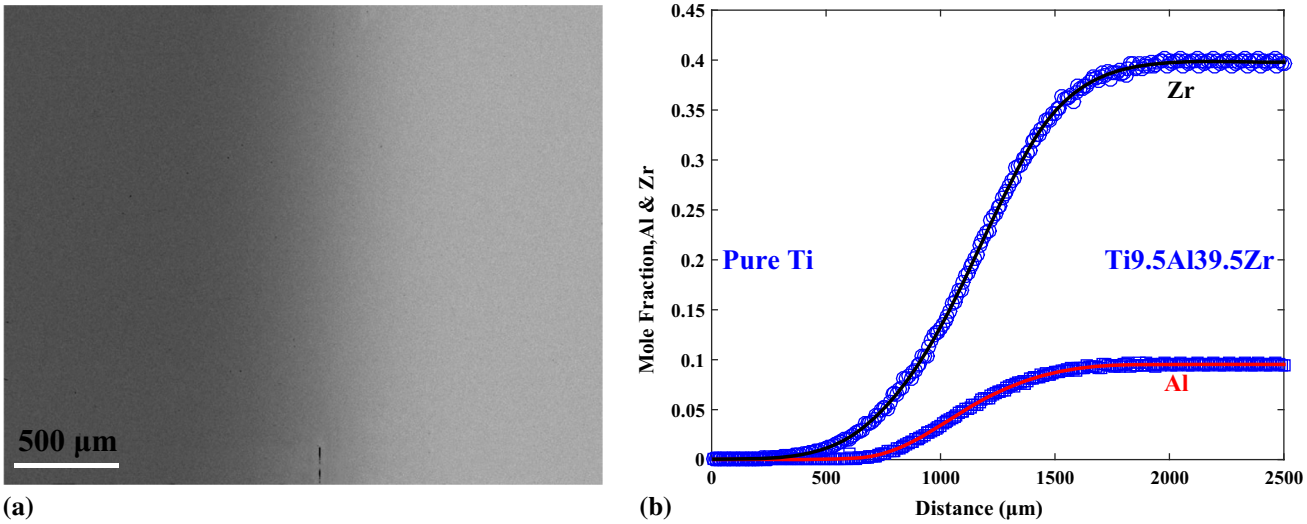

Fig. 1 Cross-sectional BSE micrograph (a) and composition profiles (b) of diffusion couple A7 at 1273 K for 48 h. The symbols are EPMA measurements

$$x(z) = \sum_i a_i \mathrm{erf}[b_i z - c_i], \qquad \text{(Eq 1)}$$

where $x(z)$ represents the composition at the distance z, a, b, and c are the adjustable parameters, and i is typically up to 4 depending on the details of composition profiles of the diffusion couple.

To avoid the need of locating the Matano plane in the well-known Matano-Kirkaldy method,[20] that may introduce a source of some uncertainty, the Whittle-Green (W-G)[21] method was utilized to extract ternary interdiffusion coefficients. The W-G method introduces a normalized composition variable: $Y = \frac{x - x_L}{x_R - x_L}$, where x_L and x_R represent the compositions at the left and right ends, respectively.[22] For the Ti-Al-Zr ternary system, Fick's second law can be expressed with the W-G method as:

$$\frac{1}{2t}\left(\frac{\mathrm{d}z}{\mathrm{d}Y_{\mathrm{Al}}}\right)_z \left[(1 - Y_{\mathrm{Al}}) \int_{-\infty}^{z} Y_{\mathrm{Al}}\mathrm{d}z + Y_{\mathrm{Al}} \int_{z}^{+\infty} (1 - Y_{\mathrm{Al}})\mathrm{d}z\right] = \tilde{D}^{\mathrm{Ti}}_{\mathrm{AlAl}} + \tilde{D}^{\mathrm{Ti}}_{\mathrm{AlZr}} \frac{\mathrm{d}x_{\mathrm{Zr}}}{\mathrm{d}x_{\mathrm{Al}}}, \qquad \text{(Eq 2a)}$$

$$\frac{1}{2t}\left(\frac{\mathrm{d}z}{\mathrm{d}Y_{\mathrm{Zr}}}\right)_z \left[(1 - Y_{\mathrm{Zr}}) \int_{-\infty}^{z} Y_{\mathrm{Zr}}\mathrm{d}z + Y_{\mathrm{Zr}} \int_{z}^{+\infty} (1 - Y_{\mathrm{Zr}})\mathrm{d}z\right] = \tilde{D}^{\mathrm{Ti}}_{\mathrm{ZrZr}} + \tilde{D}^{\mathrm{Ti}}_{\mathrm{ZrAl}} \frac{\mathrm{d}x_{\mathrm{Al}}}{\mathrm{d}x_{\mathrm{Zr}}}, \qquad \text{(Eq 2b)}$$

where $\tilde{D}^{\mathrm{Ti}}_{\mathrm{AlAl}}$ and $\tilde{D}^{\mathrm{Ti}}_{\mathrm{ZrZr}}$ are the main interdiffusion coefficients, $\tilde{D}^{\mathrm{Ti}}_{\mathrm{AlZr}}$ and $\tilde{D}^{\mathrm{Ti}}_{\mathrm{ZrAl}}$ are the cross ones, respectively. All four interdiffusion coefficients can be obtained by simultaneously solving a set of four equations of Eq 2a and 2b resulting from one pair of diffusion couples whose diffusion paths intersect at a common composition.

The impurity diffusion coefficients of Al in BCC Ti-Zr and Zr in BCC Ti-Al binary alloys were computed from composition profiles of the A1-A6 and B1-B6 couples by using the generalized Hall method.[23] Similar to its binary protocol, the profiles were first transformed to a plot of μ versus λ, wherein $\mu = \mathrm{erf}^{-1}(2Y - 1)$ and $\lambda = x/\sqrt{t}$. By fitting the plot with a linearity $\mu = h\lambda + k$, the impurity diffusion coefficients on the left and right terminal compositions can be obtained by Eq 3a and 3b respectively, with knowing the linear fit coefficients h_1 and k_1 for the left side, and h_2 and k_2 for the right side of the diffusion couples,

$$\tilde{D}(x') = \frac{1}{4h_1^2}\left[1 + \frac{2k_1}{\sqrt{\pi}}\exp(\mu^2) \times Y(x')\right], \qquad \text{(Eq 3a)}$$

$$\tilde{D}(x') = \frac{1}{4h_2^2}\left\{1 - \frac{2k_2}{\sqrt{\pi}}\exp(\mu^2)[1 - Y(x')]\right\}, \qquad \text{(Eq 3b)}$$

where x' is the terminal composition.

3 Experimental Results

3.1 Composition Profiles and Diffusion Paths

Figure 2 shows two sets of the representative composition profiles of the diffusion couples fabricated in this work, i.e. the ternary couples A5 and A7 at 1273 K (1000 °C) for 48 h and the couples B2 and B9 at 1473 K (1200 °C) for 17 h. It is apparent that the diffusion penetrations of Al and Zr, in a typical S-shape, approximately range 1.5 and 2.0 mm (see Fig. 2a) at 1273 K (1000 °C), and 2.2 and 2.5 mm (see Fig. 2b) at 1473 K (1200 °C), respectively. It thus implies that Zr diffuses in the BCC Ti-Al-Zr alloys at

a rate faster that Al (i.e. being around 1.8 times), and the difference between Al and Zr decreases (from 1.8 to 1.2 times) when temperature rises.

Figure 3 maps the diffusion paths of the Ti-Al-Zr ternary couples at 1273 K (1000 °C) and 1473 K (1200 °C) in the ternary Gibbs' isotherms. The diffusion paths at both the temperatures are clearly S-shaped, however, their appearance differs at the two temperatures. At lower temperature of 1273 K (1000 °C), the ends of majority of the diffusion paths tend to be parallel to the direction at a constant Al content, i.e. the Ti-Zr vicinity, concludes Al as a slower diffuser,[24] while at higher temperature of 1473 K (1200 °C), the end direction deviates, implying that Zr and Al tend to diffuse at the comparable rates.

3.2 Diffusion Coefficients

The interdiffusion coefficients extracted at the intersection compositions of the diffusion paths are summarized in Table 2 for 1273 K (1000 °C) and Table 4 for 1473 K (1200 °C).[22,25] Note that the standard deviations were determined from the independent calculations upon five ERFEX representation treatments with the EPMA data. The reliability of the obtained diffusion coefficients was

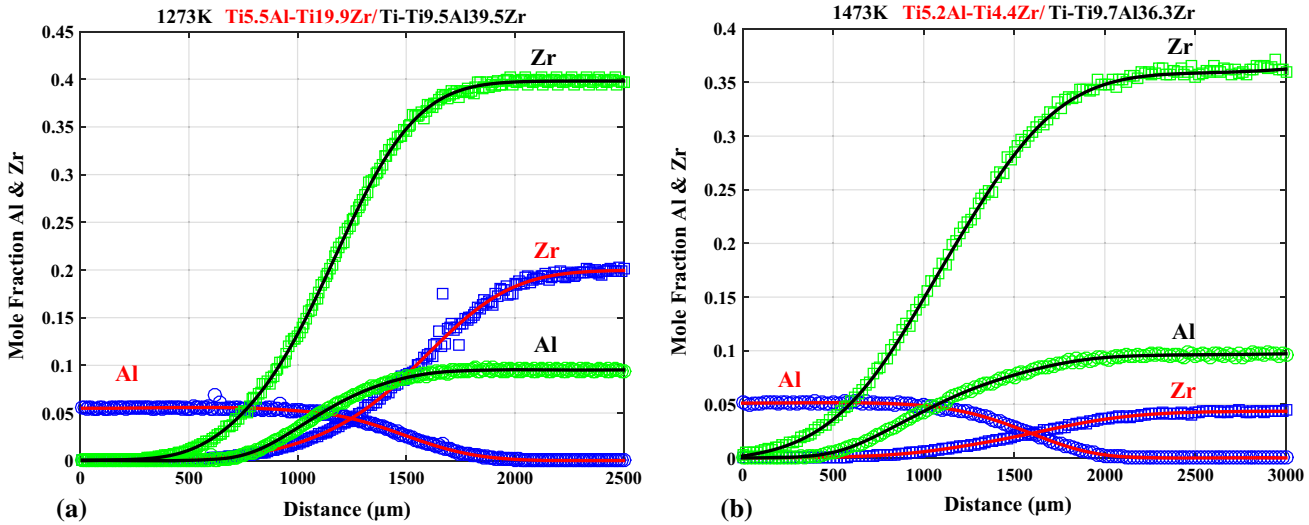

Fig. 2 Composition profiles of Ti-Al-Zr couples, (a) A5-A7 at 1273 K for 48 h, (b) B2-B9 at 1473 K for 17 h. The symbols are EPMA data, and the curves are the analytical ERFEX forms

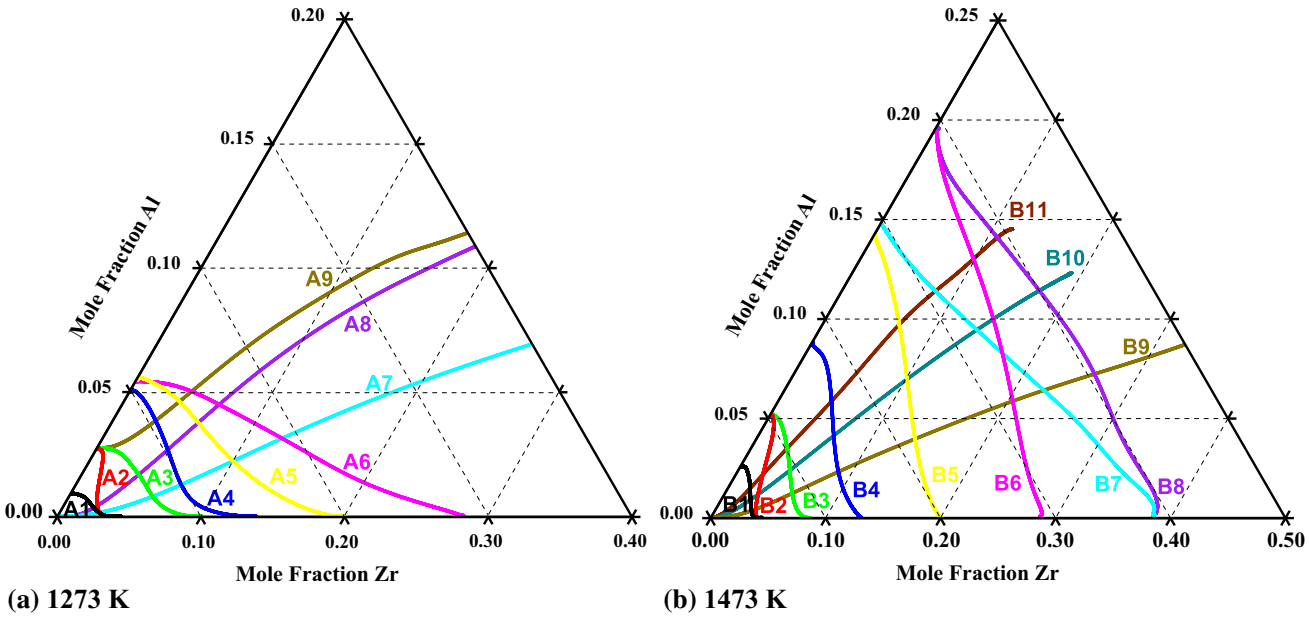

Fig. 3 Diffusion paths for Ti-Al-Zr couples annealed at (a) 1273 K for 48 h, (b) 1473 K for 17 h

Table 2 Experiment diffusion coefficients of BCC Ti-Al-Zr alloys at 1273 K (1000 °C)

Diffusion couple	Composition, at.%		Interdiffusion coefficients (10^{-13} m^2 s^{-1})			
	Al	Zr	$\tilde{D}^{Ti}_{AlAl}$	$\tilde{D}^{Ti}_{AlZr}$	$\tilde{D}^{Ti}_{ZrZr}$	$\tilde{D}^{Ti}_{ZrAl}$
A1-A7	0.2	2.8	1.3 ± 0.1	0.02 ± 0.1	3.8 ± 0.1	− 5.3 ± 0.4
A1-A8	0.4	2.2	1.1 ± 0.1	− 0.1 ± 0.1	4.6 ± 0.1	− 1.3 ± 0.2
A2-A7	0.2	2.8	1.3 ± 0.1	0.02 ± 0.1	3.6 ± 0.1	− 4.0 ± 0.4
A2-A8	0.4	2.3	1.2 ± 0.1	− 0.1 ± 0.1	4.6 ± 0.1	− 0.9 ± 0.1
A3-A7	0.8	5.8	1.4 ± 0.1	− 0.03 ± 0.1	3.8 ± 0.1	− 1.7 ± 0.2
A3-A8	1.7	4.0	1.4 ± 0.1	− 0.1 ± 0.1	4.7 ± 0.1	− 0.4 ± 0.1
A4-A7	1.3	7.4	1.4 ± 0.1	0.02 ± 0.1	3.7 ± 0.1	− 0.8 ± 0.1
A4-A8	2.7	5.0	1.5 ± 0.1	− 0.03 ± 0.1	4.2 ± 0.1	0.2 ± 0.1
A4-A9	3.9	3.0	1.6 ± 0.2	− 0.1 ± 0.1	4.2 ± 0.2	1.3 ± 0.2
A5-A7	2.3	10.1	1.8 ± 0.1	− 0.1 ± 0.1	3.6 ± 0.1	− 0.6 ± 0.1
A5-A8	3.8	6.0	1.8 ± 0.1	− 0.1 ± 0.1	4.5 ± 0.1	0.1 ± 0.1
A5-A9	4.6	3.9	1.7 ± 0.1	− 0.1 ± 0.1	5.0 ± 0.1	0.3 ± 0.1
A6-A7	3.2	12.5	1.7 ± 0.1	− 0.1 ± 0.1	3.3 ± 0.1	0.2 ± 0.2
A6-A8	4.5	6.7	1.7 ± 0.1	− 0.1 ± 0.1	3.9 ± 0.1	0.7 ± 0.1
A6-A9	5.0	4.3	1.5 ± 0.1	− 0.03 ± 0.1	4.4 ± 0.1	1.0 ± 0.1
Average	2.3	5.3	1.5	− 0.1	4.1	− 0.8

Table 3 Experiment diffusion coefficients of BCC Ti-Al-Zr alloys at 1473 K (1200 °C)

Diffusion couple	Composition, at.%		Interdiffusion coefficients (10^{-13} m^2 s^{-1})			
	Al	Zr	$\tilde{D}^{Ti}_{AlAl}$	$\tilde{D}^{Ti}_{AlZr}$	$\tilde{D}^{Ti}_{ZrZr}$	$\tilde{D}^{Ti}_{ZrAl}$
B1-B9	0.4	3.2	6.2 ± 0.3	0.3 ± 0.2	16.8 ± 0.2	− 1.6 ± 0.9
B1-B10	0.9	2.6	6.3 ± 0.1	− 0.2 ± 0.1	14.3 ± 0.1	− 2.2 ± 0.1
B1-B11	1.5	1.9	6.3 ± 0.1	− 1.2 ± 0.2	16.7 ± 0.1	− 1.9 ± 0.1
B2-B9	0.5	3.5	6.2 ± 0.2	0.3 ± 0.2	16.6 ± 0.3	− 0.3 ± 0.5
B2-B10	1.2	2.9	6.7 ± 0.1	− 0.2 ± 0.1	14.3 ± 0.2	− 2.1 ± 0.2
B2-B11	2.2	2.4	6.9 ± 0.1	− 1.1 ± 0.1	16.6 ± 0.5	− 1.8 ± 0.3
B3-B9	1.2	5.9	9.0 ± 0.1	0.1 ± 0.1	17.6 ± 0.2	− 0.9 ± 0.5
B3-B10	2.4	4.5	8.7 ± 0.1	− 1.1 ± 0.1	16.3 ± 0.1	− 3.5 ± 0.1
B3-B11	3.5	3.2	8.8 ± 0.1	− 1.9 ± 0.1	18.0 ± 0.2	− 2.7 ± 0.7
B4-B9	2.3	8.8	11.2 ± 0.1	0.5 ± 0.1	16.8 ± 0.1	2.8 ± 0.2
B4-B10	4.1	6.6	10.5 ± 0.1	− 0.9 ± 0.1	16.2 ± 0.2	− 2.1 ± 0.2
B4-B11	5.9	4.7	10.5 ± 0.1	− 1.6 ± 0.1	18.4 ± 0.1	− 1.6 ± 0.1
B5-B9	4.0	13.8	14.4 ± 0.1	0.2 ± 0.1	18.6 ± 0.3	1.4 ± 0.9
B5-B10	7.0	10.1	14.2 ± 0.1	− 1.9 ± 0.1	18.5 ± 0.4	− 3.3 ± 0.4
B5-B11	9.7	6.7	13.2 ± 0.1	− 4.1 ± 0.1	20.2 ± 0.6	− 2.1 ± 0.5
B6-B9	5.9	20.4	19.7 ± 0.1	− 0.1 ± 0.1	20.5 ± 0.3	− 1.7 ± 0.3
B6-B10	10.0	14.6	19.1 ± 0.5	− 3.0 ± 0.3	20.1 ± 0.2	− 4.5 ± 0.3
B6-B11	13.0	9.8	16.1 ± 0.1	− 6.5 ± 0.1	19.8 ± 0.4	− 6.2 ± 0.7
B7-B9	6.4	22.5	19.5 ± 0.3	0.3 ± 0.1	18.3 ± 0.1	8.1 ± 0.4
B7-B10	9.5	13.7	17.0 ± 0.4	− 2.0 ± 0.1	18.3 ± 0.4	− 3.0 ± 1.0
B7-B11	11.4	8.2	16.0 ± 0.1	− 2.5 ± 0.1	18.0 ± 0.1	− 5.2 ± 0.3
B8-B9	7.2	26.1	23.4 ± 0.3	− 0.4 ± 0.1	20.6 ± 0.2	− 2.8 ± 0.5
B8-B10	11.4	17.2	23.2 ± 1.0	− 3.0 ± 0.4	19.2 ± 0.6	− 7.6 ± 1.4
B8-B11	14.1	10.8	14.9 ± 0.1	− 6.5 ± 0.1	18.3 ± 0.7	− 7.8 ± 1.6
Average	5.7	9.3	12.8	− 1.5	17.9	− 2.2

Table 4 Impurity diffusion coefficients of Al in Ti-Zr and Zr in Ti-Al binary Alloys

Temperature	Composition	Impurity coefficients, m^2/s	Composition	Impurity coefficients, m^2/s
1273 K	$D^*_{Al(Ti-4.4Zr)}$	1.3×10^{-13}	$D^*_{Zr(Ti-1.0Al)}$	3.6×10^{-13}
	$D^*_{Al(Ti-9.9Zr)}$	1.7×10^{-13}	$D^*_{Zr(Ti-2.8Al)}$	3.9×10^{-13}
	$D^*_{Al(Ti-13.5Zr)}$	1.8×10^{-13}	$D^*_{Zr(Ti-5.1Al)}$	4.6×10^{-13}
	$D^*_{Al(Ti-19.9Zr)}$	1.9×10^{-13}	$D^*_{Zr(Ti-5.5Al)}$	5.1×10^{-13}
	$D^*_{Al(Ti-28.2Zr)}$	1.9×10^{-13}		
	$\overline{D^*_{Al(Ti-Zr)}}$	1.7×10^{-13}	$\overline{D^*_{Zr(Ti-Al)}}$	4.3×10^{-13}
1473 K	$D^*_{Al(Ti-4.3Zr)}$	6.8×10^{-13}	$D^*_{Zr(Ti-2.6Al)}$	16.1×10^{-13}
	$D^*_{Al(Ti-8.7Zr)}$	11.5×10^{-13}	$D^*_{Zr(Ti-5.2Al)}$	16.3×10^{-13}
	$D^*_{Al(Ti-12.9Zr)}$	11.9×10^{-13}	$D^*_{Zr(Ti-8.8Al)}$	17.2×10^{-13}
	$D^*_{Al(Ti-19.9Zr)}$	15.7×10^{-13}	$D^*_{Zr(Ti-14.2Al)}$	18.5×10^{-13}
	$D^*_{Al(Ti-28.7Zr)}$	15.9×10^{-13}	$D^*_{Zr(Ti-19.5Al)}$	21.5×10^{-13}
	$D^*_{Al(Ti-38.4Zr)}$	19.9×10^{-13}		
	$\overline{D^*_{Al(Ti-Zr)}}$	13.6×10^{-13}	$\overline{D^*_{Zr(Ti-Al)}}$	17.9×10^{-13}

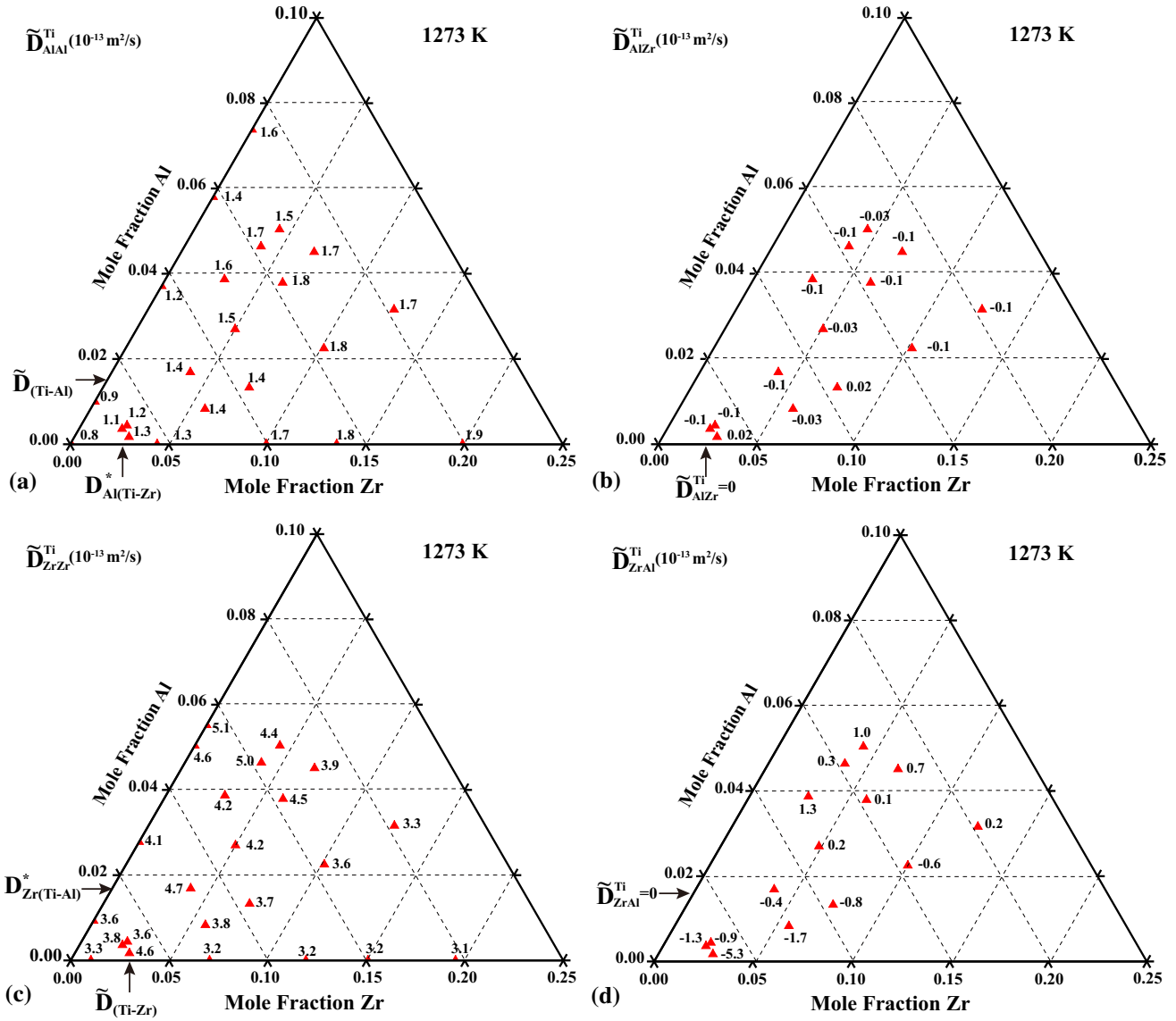

Fig. 4 Main and cross interdiffusion coefficients in BCC Ti-Al-Zr ternary alloys at 1273 K, (a) $\tilde{D}^{Ti}_{AlAl}$, (b) $\tilde{D}^{Ti}_{AlZr}$, (c) $\tilde{D}^{Ti}_{ZrZr}$, and (d) $\tilde{D}^{Ti}_{ZrAl}$

validated by checking if the thermodynamic constraints derived by Kirkaldy[26] are satisfied, i.e.

$$\tilde{D}^{Ti}_{AlAl} + \tilde{D}^{Ti}_{ZrZr} > 0, \quad \text{(Eq 4a)}$$

$$\tilde{D}^{Ti}_{AlAl}\tilde{D}^{Ti}_{ZrZr} - \tilde{D}^{Ti}_{AlZr}\tilde{D}^{Ti}_{ZrAl} \geq 0, \quad \text{(Eq 4b)}$$

$$(\tilde{D}^{Ti}_{AlAl} + \tilde{D}^{Ti}_{ZrZr})^2 \geq 4\left(\tilde{D}^{Ti}_{AlAl}\tilde{D}^{Ti}_{ZrZr} - \tilde{D}^{Ti}_{AlZr}\tilde{D}^{Ti}_{ZrAl}\right). \quad \text{(Eq 4c)}$$

As shown in Tables 2 and 3, the main interdiffusion coefficients $\tilde{D}^{\mathrm{Ti}}_{\mathrm{AlAl}}$ and $\tilde{D}^{\mathrm{Ti}}_{\mathrm{ZrZr}}$ are much larger than the cross coefficients $\tilde{D}^{\mathrm{Ti}}_{\mathrm{AlZr}}$ and $\tilde{D}^{\mathrm{Ti}}_{\mathrm{ZrAl}}$ (approximately 8 and 9 times, respectively). As usual, the cross coefficients exhibit some scattering, and are believed to have low accuracy because of the inherent error when solving Fick's second law to extract the interdiffusion coefficients. At 1273 K (1000 °C), $\tilde{D}^{\mathrm{Ti}}_{\mathrm{AlAl}}$ ranges from 1.1×10^{-13} $\mathrm{m^2/s}$ to 1.8×10^{-13} $\mathrm{m^2/s}$ with the average value being 1.5×10^{-13} $\mathrm{m^2/s}$, whereas the average of $\tilde{D}^{\mathrm{Ti}}_{\mathrm{ZrZr}}$ is 4.1×10^{-13} $\mathrm{m^2/s}$, confirming the above-stated finding that Zr indeed diffuses faster than Al. It is also apparent that both $\tilde{D}^{\mathrm{Ti}}_{\mathrm{AlAl}}$ and $\tilde{D}^{\mathrm{Ti}}_{\mathrm{ZrZr}}$ have a weak compositional dependence. On contrast, the average value of $\tilde{D}^{\mathrm{Ti}}_{\mathrm{AlAl}}$ is 12.8×10^{-13} $\mathrm{m^2/s}$ versus 19.8×10^{-13} $\mathrm{m^2/s}$ of $\tilde{D}^{\mathrm{Ti}}_{\mathrm{ZrZr}}$ at 1473 K (1200 °C), proving that the difference of diffusion rate between Al and Zr becomes smaller and is no longer three times. This is largely because $\tilde{D}^{\mathrm{Ti}}_{\mathrm{AlAl}}$ strongly increase with increasing the Zr content at higher temperature.

The impurity diffusion coefficients of Zr in binary Ti-Al alloys $D^{*}_{\mathrm{Zr(Ti-Al)}}$ and of Al in Ti-Zr alloys $D^{*}_{\mathrm{Al(Ti-Zr)}}$ were extracted from the A1-A6 and B1-B8 couples by generalized Hall method, respectively. The values listed in Table 4

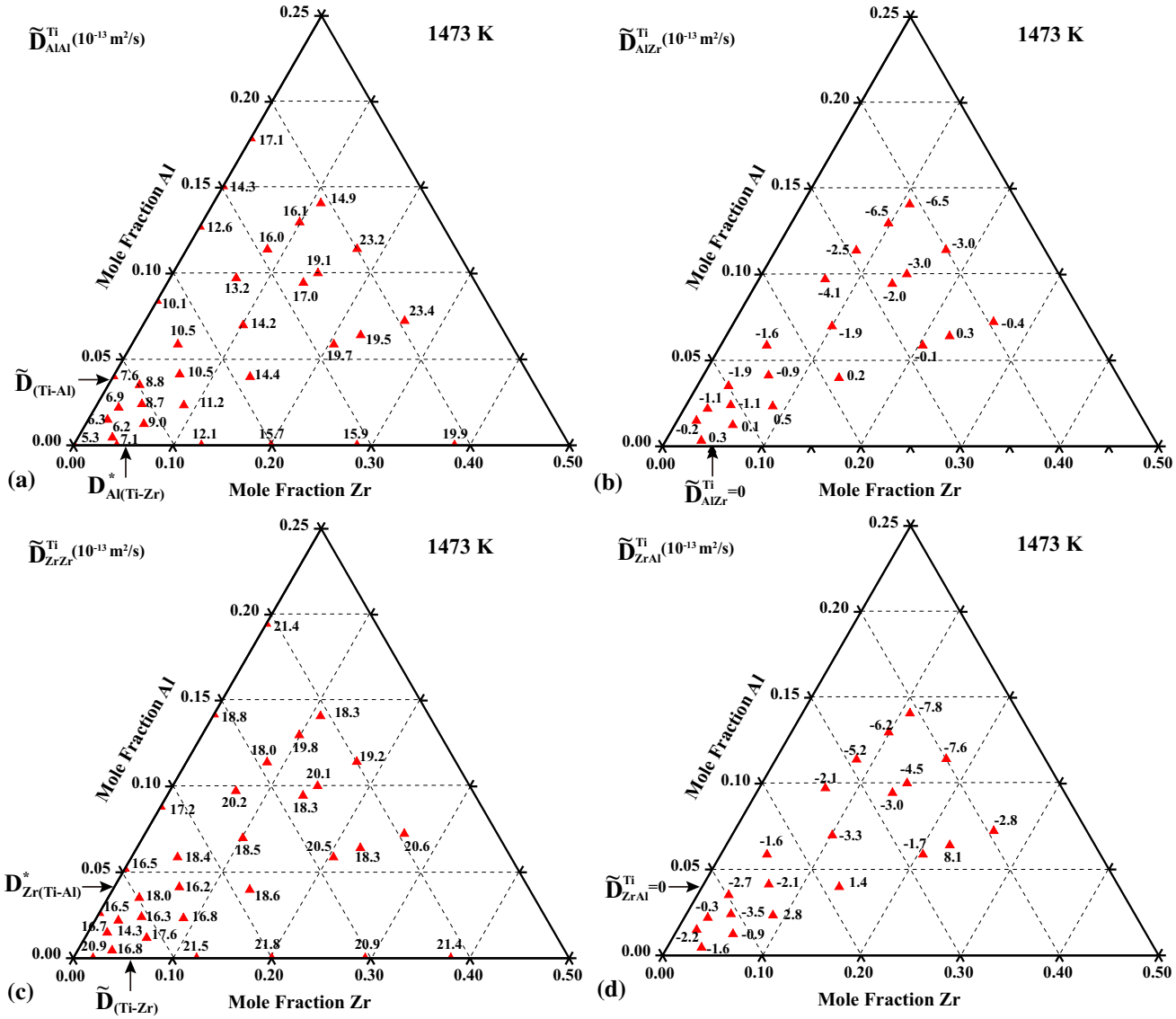

Fig. 5 Main and cross interdiffusion coefficients in BCC Ti-Al-Zr ternary alloys at 1473 K, (a) $\tilde{D}^{\mathrm{Ti}}_{\mathrm{AlAl}}$, (b) $\tilde{D}^{\mathrm{Ti}}_{\mathrm{AlZr}}$, (c) $\tilde{D}^{\mathrm{Ti}}_{\mathrm{ZrZr}}$, and (d) $\tilde{D}^{\mathrm{Ti}}_{\mathrm{ZrAl}}$

depict that both $D^{*}_{Al(Ti-Zr)}$ and $D^{*}_{Zr(Ti-Al)}$ increase with increasing the content of Al and Zr, respectively.

4 Discussions

4.1 Composition Dependence of Interdiffusion Coefficients

The extracted ternary interdiffusion coefficients are plotted in Fig. 4 for 1273 K (1000 °C) and Fig. 5 for 1473 K (1200 °C), respectively. As pointed out by Shuck and Toor,[27] the relation between the limit of the main diffusion coefficient $\tilde{D}^{k}_{ii}$ in the i-k vicinity and binary interdiffusion coefficient $\tilde{D}_{k-i}$ in the i-k binary is

$$\lim_{x_j \to 0} \tilde{D}^{k}_{ii} = \tilde{D}_{k-i}, \quad \text{(Eq 5)}$$

and between the main diffusion coefficients $\tilde{D}^{k}_{ii}$ in the j-k vicinity and the impurity diffusion coefficients $\tilde{D}^{*}_{i(j-k)}$ in the j-k binary alloy, i.e.,

$$\lim_{x_i \to 0} \tilde{D}^{k}_{ii} = D^{*}_{i(j-k)}. \quad \text{(Eq 6)}$$

It therefore yields in the Ti-Al-Zr ternary that $\tilde{D}^{Ti}_{AlAl}$ is degenerated to the binary Ti-Al interdiffusion coefficient $\tilde{D}_{Ti-Al}$ as the Zr content approaches zero and to $\tilde{D}^{*}_{Al(Ti-Zr)}$ as Al goes to zero. Likewise, $\tilde{D}^{Ti}_{ZrZr}$ becomes $\tilde{D}_{Ti-Zr}$ and $\tilde{D}^{*}_{Zr(Ti-Al)}$ as Al and Zr approach to zero, respectively. Concerning the cross coefficients, it yields $\lim_{x_i \to 0} \tilde{D}^{k}_{ij} = 0$ as the content of diffusing element is negligible. By additionally including the binary diffusion data of $\tilde{D}_{(Ti-Al)}$[12,13,28] and $\tilde{D}_{(Ti-Zr)}$[14] and the present impurity diffusion coefficients, it allows to map the broader composition dependence of the diffusion coefficients. A rough composition dependence could be thus outlined, for

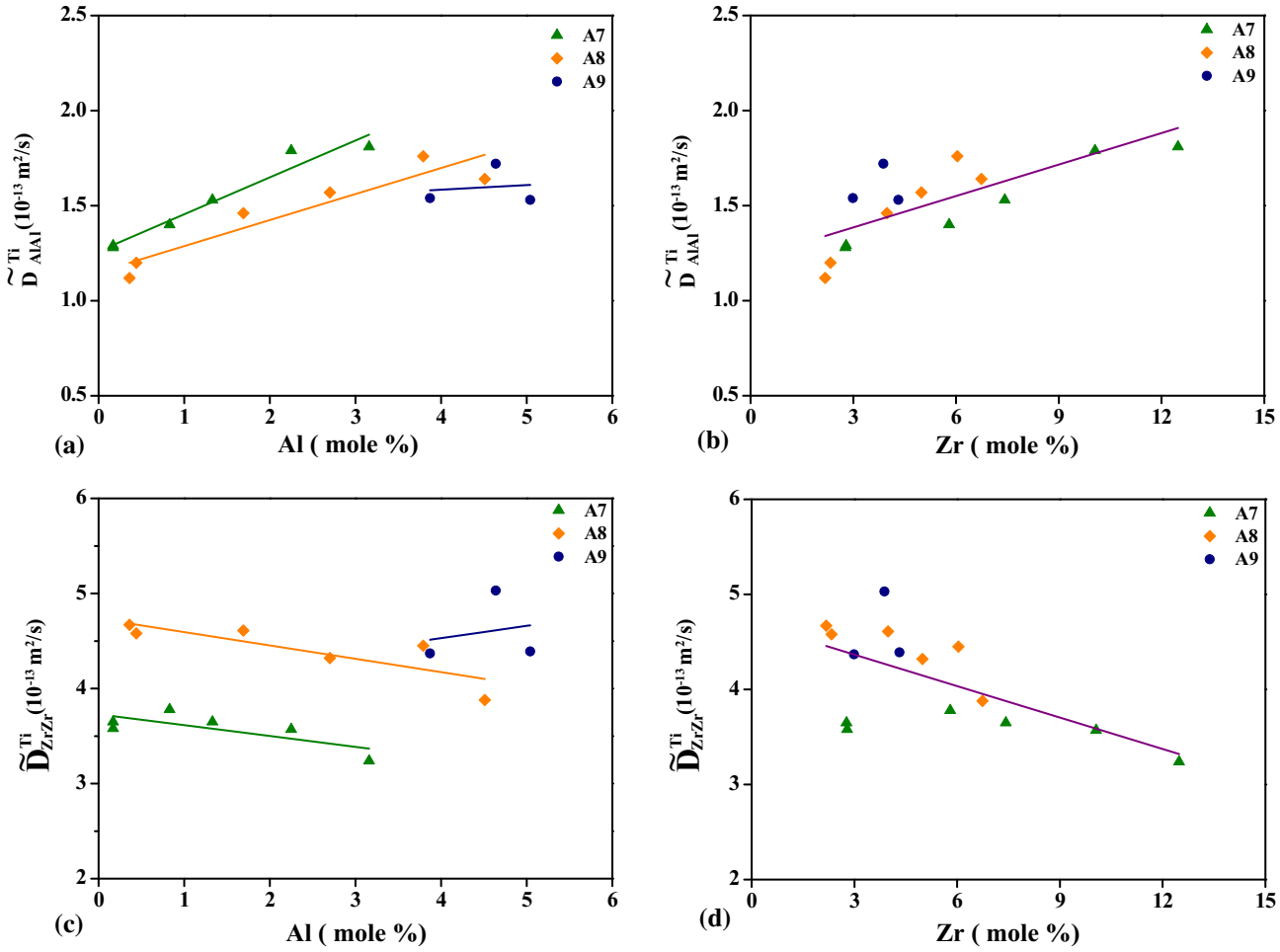

Fig. 6 The variation of ternary interdiffusion coefficients with the compositions at 1273 K. (a) $\tilde{D}^{Ti}_{AlAl}$ with Al; (b) $\tilde{D}^{Ti}_{AlAl}$ with Zr; (c) $\tilde{D}^{Ti}_{ZrZr}$ with Al; (d) $\tilde{D}^{Ti}_{ZrZr}$ with Zr

specific, at 1273 K (1000 °C), the dependence of all four interdiffusion coefficients on the Al and Zr contents is weak and ambiguous. As for 1473 K (1200 °C), while the dependence of $\tilde{D}^{\mathrm{Ti}}_{\mathrm{ZrZr}}$ on the Al and Zr contents remains weak, $\tilde{D}^{\mathrm{Ti}}_{\mathrm{AlAl}}$ has strong dependence on the Zr content, i.e. significantly increases with adding Zr.

The compositional dependence of all the interdiffusion coefficients could be quantified by illustrating the variation of the main interdiffusion coefficients $\tilde{D}^{\mathrm{Ti}}_{\mathrm{AlAl}}$ and $\tilde{D}^{\mathrm{Ti}}_{\mathrm{ZrZr}}$ with the compositions of Al and Zr at 1273 K (1000 °C) and 1473 K (1200 °C) in Fig. 6 and 7. It now becomes clearly that $\tilde{D}^{\mathrm{Ti}}_{\mathrm{AlAl}}$ increases with increasing the content of either Al or Zr, and the increase appears more considerably at the higher temperature. However, $\tilde{D}^{\mathrm{Ti}}_{\mathrm{ZrZr}}$ was noticed to decrease with the increase of Al and Zr contents at 1273 K (1000 °C) while presents an increasing trend at 1473 K (1200 °C). These distinct variations of the main interdiffusion coefficients with respect to compositions are consistent with the interdiffusion in the BCC Ti-Zr[14] and Ti-Mn binary alloys,[19] which are very likely due to the thermodynamic contribution (via thermodynamic factor) varying with the composition in the ternary system to the interdiffusion coefficients.

4.2 Temperature Dependence of Inter- and Impurity Diffusion Coefficients

By comparing the average values of the main inter- and impurity diffusion coefficients, it yields $\overline{\tilde{D}^{\mathrm{Ti}}_{\mathrm{AlAl}}}/\overline{\tilde{D}^{\mathrm{Ti}}_{\mathrm{ZrZr}}}(1273K) = 0.37$, $\overline{\tilde{D}^{\mathrm{Ti}}_{\mathrm{AlAl}}}/\overline{\tilde{D}^{\mathrm{Ti}}_{\mathrm{ZrZr}}}(1473K) = 0.71$, $\overline{\tilde{D}^{*}_{\mathrm{Zr(Ti-Al)}}}/\overline{\tilde{D}^{*}_{\mathrm{Al(Ti-Zr)}}}(1273K) = 0.37$, $\frac{\overline{\tilde{D}^{*}_{\mathrm{Zr(Ti-Al)}}}}{\overline{\tilde{D}^{*}_{\mathrm{Al(Ti-Zr)}}}(1473K)} = 0.66$. In addition, the average values of diffusion coefficients at 1273 K (1000 °C) and 1473 K (1200 °C) were also compared as follows, $\overline{\tilde{D}^{\mathrm{Ti}}_{\mathrm{AlAl}}}(1473K)/\overline{\tilde{D}^{\mathrm{Ti}}_{\mathrm{AlAL}}}(1273K) = 8.50$, $\overline{\tilde{D}^{\mathrm{Ti}}_{\mathrm{ZrZr}}}(1473K)/\overline{\tilde{D}^{\mathrm{Ti}}_{\mathrm{ZrZr}}}(1273K) = 4.36$, $\overline{D^{*}_{\mathrm{Al(Ti-Zr)}}}(1473K)/\overline{D^{*}_{\mathrm{Al(Ti-Zr)}}}(1273K) = 7.06$, $\overline{D^{*}_{\mathrm{Zr(Ti-Al)}}}(1473K)/\overline{D_{\mathrm{Zr(}}}$

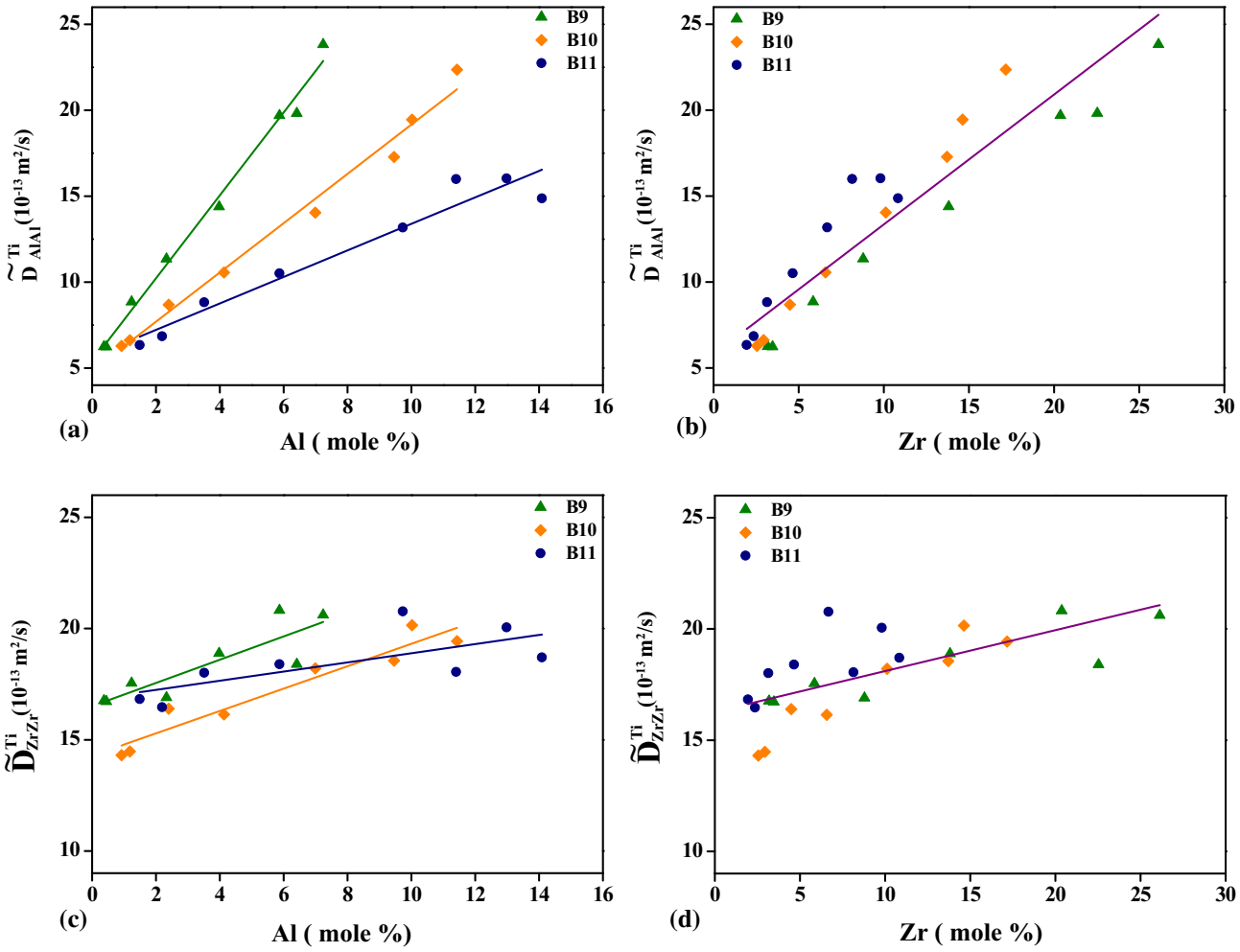

Fig. 7 The variation of ternary interdiffusion coefficients with the compositions at 1473 K. (a) $\tilde{D}^{\mathrm{Ti}}_{\mathrm{AlAl}}$ with Al; (b) $\tilde{D}^{\mathrm{Ti}}_{\mathrm{AlAl}}$ with Zr; (c) $\tilde{D}^{\mathrm{Ti}}_{\mathrm{ZrZr}}$ with Al; (d) $\tilde{D}^{\mathrm{Ti}}_{\mathrm{ZrZr}}$ with Zr

Table 5 Average main interdiffusion coefficients in Ti-Al-X ternary systems (Ni, Co, Fe, Mn, Zr, Cr, Sn, V, Nb, and Mo) at 1473 K

	Average $\tilde{D}^{\mathrm{Ti}}_{\mathrm{AlAl}}$, m^2/s	Average $\tilde{D}^{\mathrm{Ti}}_{\mathrm{XX}}$, m^2/s
Ti-Al-Ni	1.9×10^{-12}	2.2×10^{-11}
Ti-Al-Co	1.3×10^{-12}	1.9×10^{-11}
Ti-Al-Fe	1.3×10^{-12}	1.2×10^{-11}
Ti-Al-Mn	1.3×10^{-12}	3.1×10^{-12}
Ti-Al-Zr	1.3×10^{-12}	1.8×10^{-12}
Ti-Al-Cr	7.4×10^{-13}	1.6×10^{-12}
Ti-Al-Sn	9.2×10^{-13}	8.2×10^{-13}
Ti-Al-V	6.8×10^{-13}	4.1×10^{-13}
Ti-Al-Nb	6.2×10^{-13}	4.0×10^{-13}
Ti-Al-Mo	4.5×10^{-13}	1.5×10^{-13}

$\mathrm{Ti}-\mathrm{Al})^{*}(1273K) = 4.02$. The findings obviously clarify that the temperature dependence is noticeable.

4.3 Ti-Al-X Ternaries

A systematic comparison of the average main interdiffusion coefficients at 1473 K (1200 °C) in ten Ti-Al-X (Ni,[29] Co,[30] Fe,[31] Mn,[19] Zr, Cr,[32] Sn,[18] V,[33] Nb,[27] Mo[24]) ternary systems is presented in Table 5. The diffusion rate of Zr is one order of magnitude smaller than the fast diffusers (i.e. Ni, Co, and Fe) and is one order magnitude greater than the refractory metals (i.e. V, Nb, and Mo). It reveals that the order of the average main interdiffusion coefficient $\overline{\tilde{D}^{\mathrm{Ti}}_{\mathrm{XX}}}$ could be expressed as $D_{\mathrm{Ni}} > D_{\mathrm{Co}} > D_{\mathrm{Fe}} > D_{\mathrm{Mn}} > D_{\mathrm{Zr}} > D_{\mathrm{Cr}} > D_{\mathrm{Sn}} > D_{\mathrm{V}} > D_{\mathrm{Nb}} > D_{\mathrm{Mo}}$, thus the Zr diffusion is comparable to that of Cr. Previous reports demonstrated that the diffusion of Ni, Co, and Fe in BCC Ti alloys is of the interstitial nature or by a mixed vacancy-interstitial mechanism[18,31,34]). The Zr diffusion in the Ti-Al-X ternary should thus occur via a normal vacancy mechanism like Cr, Sn, V, Nb, and Mo, however, the Al diffusion is significantly promoted by the presence of Zr.

5 Conclusions

In brief, diffusion behavior in BCC Ti-Al-Zr ternary alloys was investigated at 1273 K (1000 °C) and 1473 K (1200 °C) by using the solid-state diffusion couple technique. The ternary inter- and impurity diffusion coefficients were extracted by the Whittle-Green and generalized Hall methods, respectively. The results are summarized as follows:

1. $\tilde{D}^{\mathrm{Ti}}_{\mathrm{AlAl}}$ increases with increasing the content of either Al or Zr, and the increase is appearing more considerably at the higher temperature. However, $\tilde{D}^{\mathrm{Ti}}_{\mathrm{ZrZr}}$ was noticed to decrease with the increase of Al and Zr contents at 1273 K (1000 °C) while there is an upward trend at 1473 K (1200 °C). Due to the relatively large scattering, the composition dependence of the cross interdiffusion coefficients is ambiguous.
2. The impurity diffusion coefficients $D^{*}_{\mathrm{Al(Ti-Zr)}}$ and $D^{*}_{\mathrm{Zr(Ti-Al)}}$ increase with increasing the content of alloying element at both 1273 K (1000 °C) and 1473 K (1200 °C).
3. A complete comparison of ten Ti-Al-X (Ni, Co, Fe, Mn, Zr, Cr, Sn, V, Nb, and Mo) ternary systems was made with the average main interdiffusion coefficient $\overline{\tilde{D}^{\mathrm{Ti}}_{\mathrm{XX}}}$. It exhibits $D_{\mathrm{Ni}} > D_{\mathrm{Co}} > D_{\mathrm{Fe}} > D_{\mathrm{Mn}} > D_{\mathrm{Zr}} > D_{\mathrm{Cr}} > D_{\mathrm{Sn}} > D_{\mathrm{V}} > D_{\mathrm{Nb}} > D_{\mathrm{Mo}}$, and the Zr diffusion is most comparable to Cr, suggesting it is a vacancy-controlled mechanism.

Acknowledgments This research was funded by the Defense Industrial Technology Development Program of China [No. JCKY2018414C020]. YC acknowledges the support from the Natural Science Funds of China [Grant No. 51571113]. GX was funded by the Natural Science Funds of China [Grant No. 51701094] and the Natural Science Funds of Jiangsu Province [Grant No. BK20171014]. FF and YG would like to thank the support from the Synergetic Innovation Center for Advanced Materials, Jiangsu Collaborative Innovation Center for Advanced Inorganic Function Composites, Nanjing Tech University.

References

1. G. Lütjering and J.C. Williams, *Titanium Based Intermetallics*, Springer, Berlin, 2003
2. R.R. Boyer, Attributes, Characteristics, and Applications of Titanium and Its Alloys, *JOM*, 2010, **62**(5), p 21-24
3. R.R. Boyer and R.D. Briggs, The Use of β Titanium Alloys in the Aerospace Industry, *J. Mater. Eng. Perform.*, 2005, **14**(6), p 681-685
4. J.H. Xiong, S.K. Li, F.Y. Gao, and J.X. Zhang, Microstructure and Mechanical Properties of Ti6321 Alloy Welded Joint by GTAW, *Metall. Trans. A*, 2015, **640**, p 419-423
5. X. Zhang, H.C. Kou, J.S. Li, F.S. Zhang, and L. Zhou, Evolution of the Secondary α Phase Morphologies During Isothermal Heat Treatment in Ti-7333 Alloy, *J. Alloys Compd.*, 2013, **577**(2–3), p 516-522
6. Y.L. Wang, S.X. Hui, R. Liu, and W.J. Ye, Evaluation of dynamic performance and ballistic behavior of Ti-5Al-5Mo-5V-3Cr-1Zr alloy, *Trans. Nonferrous Met. Soc.*, 2015, **25**(2), p 429-436
7. H. Chang, E. Gautier, F. Bruneseaux, and L. Zhou, β → α+β Isothermal Phase Transformation Kinetics in Ti-B19 Metastable Titanium Alloy, *Rare Metal Mat. Eng.*, 2006, **35**(11), p 1696-1699
8. G.J. Fan, X.P. Song, M.X. Quan, and Z.Q. Hu, Mechanical Alloying and Thermal Stability of Al 67 Ti 25M 8 (M = Cr, Zr, Cu), *Metall. Trans. A*, 1997, **231**(1–2), p 111-116
9. L. Feng, J.S. Li, Y.W. Cui, L. Huang, H.C. Kou, and L. Zhou, Research on Interdiffusion Behavior of Ti-Zr Binary Alloy in the β Phase, *Rare Met. Mater. Eng.*, 2011, **40**(04), p 610-614

10. Q. Chen, N. Ma, K.S. Wu, and Y.Z. Wang, Quantitative Phase Field Modeling of Diffusion-Controlled Precipitate Growth and Dissolution in Ti-Al-V, *Scr. Mater.*, 2004, **50**(4), p 471-476
11. H. Hu and S.A. Argyropoulos, Mathematical Modelling of Solidification and Melting: A Review, *Model. Simul. Mater. Sci. Eng.*, 1996, **4**, p 371-396
12. H. Araki, T. Yamane, Y. Minamino, S. Saji, Y. Hana, and S.B. Jung, Anomalous Diffusion of Aluminum in β-Titanium, *Metall. Trans. A*, 1994, **25**(4), p 874-876
13. S.Y. Lee, O. Taguchi, and Y. Iijima, Diffusion of Alummum in β-Titanium, *Mater. Trans.*, 2010, **51**(10), p 1809-1813
14. I. Thibon, D. Ansel, and T. Gloriant, Interdiffusion in β-Ti-Zr Binary Alloys, *J. Alloys Compd.*, 2009, **470**(1–2), p 127-133
15. F. Yang, F.H. Xiao, S.G. Liu, S.S. Dong, L.H. Huang, Q. Chen, G.M. Cai, H.S. Liu, and Z.P. Jin, Isothermal Section of Al-Ti-Zr Ternary System at 1273K, *J. Alloys Compd.*, 2014, **585**, p 325-330
16. A.G. Nikitin, S.V. Spichak, S.V. Yu, and A.G. Naumovets, Symmetries and Modelling Functions for Diffusion Processes, *J. Phys. D*, 2009, **42**, p 55301
17. W.M. Bai, Y.Y. Tian, G.L. Xu, Z.J. Yang, L.B. Liu, P.J. Masset, and L.G. Zhang, Diffusivities and Atomic Mobilities in bcc Ti-Zr-Nb Alloys, *Calphad*, 2019, **62**, p 160-174
18. Q.J. Wu, J.Y. Wang, Y.Y. Gu, Y.H. Guo, G.L. Xu, and Y.W. Cui, Experimental Diffusion Research on BCC Ti-Al-Sn Ternary Alloys, *J. Phase Equilib. Diff.*, 2018, **39**(5), p 724-730
19. X. Huang, Y.J. Tan, Y.H. Guo, G.L. Xu, and Y.W. Cui, Experimental Diffusion Research on BCC Ti-Mn Binary and Ti-Al-Mn Ternary Alloys, *J. Phase Equilib. Diffus.*, 2018, **39**(5), p 702-713
20. J.S. Kirkaldy, Diffusion in Multicomponent Metallic Systems, *Can. J. Phys.*, 1957, **35**(4), p 435-440
21. D.P. Whittle and A. Green, The Measurement of Diffusion Coefficients in Ternary Systems, *Scr. Mater.*, 1974, **8**(7), p 883-884
22. C.Y. Wang, G.L. Xu, and Y.W. Cui, Mapping of Diffusion and Nanohardness Properties of Fcc Co-Al-V Alloys Using Ternary Diffusion Couples, *Metall. Trans. A*, 2017, **48**(9), p 4286-4296
23. L.D. Hall, An Analytical Method of Calculating Variable Diffusion Coefficients, *J. Chem. Phys.*, 1953, **21**, p 87-89
24. Y. Chen, B. Tang, G.L. Xu, C.Y. Wang, H.C. Kou, J.S. Li, and Y.W. Cui, Diffusion Research in BCC Ti-Al-Mo Ternary Alloys, *Metall. Mater. Trans. A*, 2014, **45A**(4), p 1647-1652
25. Y. Chen, J.S. Li, B. Tang, G.L. Xu, H.C. Kou, and Y.W. Cui, Interdiffusion in FCC Co-Al-Ti Ternary Alloys, *J. Phase Equilib. Diff.*, 2015, **36**(2), p 127-135
26. J.S. Kirkaldy, D. Weichert, and Z.U. Haq, Diffusion in Multicomponent Metallic Systems: VI. Some Thermodynamic Properties of the D Matrix and the Corresponding Solutions of the Diffusion Equations, *Can. J. Phys.*, 1963, **41**(12), p 2166-2173
27. F.O. Shuck and H.L. Toor, Diffusion in the Three Component Liquid System Methyl Alcohol-n-Propyl Alcohol-Isobutyl Alcohol, *J. Phys. Chem.*, 1963, **67**(3), p 540-545
28. Y.Y. Gu, F.J. Fan, Y.H. Guo, G.L. Xu, H. Chang, L. Zhou, and Y.W. Cui, Diffusion and Atomic Mobility of BCC Ti-Al-Nb Alloys: Experimental Determination and Computational Modeling, *Calphad*, 2018, **62**, p 83-91
29. B. Gao, Y.Y. Gu, Q.J. Wu, Y.H. Guo, and Y.W. Cui, Diffusion Research in BCC Ti-Al-Ni Ternary Alloys, *J. Phase Equilib. Diff.*, 2017, **38**(4), p 502-508
30. T. Takahashi, Ternary Diffusion and Thermodynamic Interaction in the β Solid Solutions of Ti-Al-Co Alloys, *J. Jpn. Inst. Met.*, 2009, **59**(8), p 432-438
31. T. Takahashi and Y. Minamino, Ternary Diffusion and Thermodynamic Interaction in the β Solid Solutions of Ti-Al-Fe Alloys at 1423 K, *J. Alloys Compd.*, 2012, **545**, p 168-175
32. W.B. Li, B. Tang, Y.W. Cui, R. Hu, H. Chang, J.S. Li, and L. Zhou, Assessment of Diffusion Mobility for the bcc Phase of the Ti-Al-Cr System, *Calphad*, 2011, **35**, p 384-390
33. L. Huang, Y.W. Cui, H. Chang, H. Zhong, J.S. Li, and L. Zhou, Assessment of Atomic Mobilities for bcc Phase of Ti-Al-V System, *J. Phase Equilib. Diff.*, 2010, **31**(2), p 135-143
34. G.M. Hood and R.J. Schultz, Ultra-fast Solute Diffusion in α-Ti and α-Zr, *Philos. Mag.*, 1972, **26**(2), p 329-336